TriDurLE

National Center for Transportation Infrastructure Durability & Life-Extension

Project ID: 2020-MST-05

Final Report
Analyzing the Impact of Autonomous Maintenance Technology to Transportation Infrastructure Capacity for Condition Monitoring and Performance Management

By

Xianbiao Hu, Pennsylvania State University

Qing Tang, Pennsylvania State University

Jenny Liu, Missouri University of Science and Technology

for

National University Transportation Center TriDurLE
Department of Civil & Environmental Engineering
405 Spokane Street, PO Box 642910
Washington State University, Pullman, WA 99164-2910

Date

7/29/2022

Acknowledgements

Disclaimer

Table of Contents

Contents

List of Figures

List of Tables

No table of figures entries found.

Executive Summary

Work zones are critical for efficient and safe operation of a highway transportation system. Performing the maintenance required for a roadway infrastructure, however, could involve risks. In 2017 alone, a total of 158,000 total vehicle crashes occurred in our nation's work zones, accounting for 61,000 injuries [1]. Many of these frequently involved State Department of Transportation (DOT) employees. The Autonomous Maintenance Technology (AMT) is a quickly emerging autonomous-vehicle-based technology for improving transportation infrastructure maintenance by removing drivers from risk. Its impact to transportation capacity, although critically important to transportation infrastructure condition monitoring and performance management, has not been studied before. In this project, models and algorithms are developed to reveal the fundamental working mechanism of AMT, and analyze the resulted traffic flow capacity discount associated with AMT vehicles as a moving bottleneck. Newell car following model and moving-bottleneck-based traffic flow theory are utilized to mathematically derive the roadway capacity under different scenarios. The accuracy of the developed model is validated through comparison with NGSIM open dataset. The results of the proposed study provide preliminary guidance to state DOT for transportation roadway maintenance-related work, as well needed transportation performance management and system management.

Chapter 1. Introduction

1.1 Problem Statement

Work zones are critical for efficient and safe operation of a highway transportation system. Mobile and slow-moving operations (M&SMO) at work zone locations, such as striping, sweeping, bridge flushing and pothole patching, are critical for efficient and safe operation of the highway transportation system. Performing the maintenance of roadway infrastructure, however, could come with risks. In 2017 alone, a total of 158,000 total crashes occurred in our nation's work zones, accounting for 61,000 injuries with many often them involved State Department of Transportation employees [1]. How to reduce hazard to roadway workers and achieve a safer environment for both roadway maintenance operators and the public have been a challenging problem.

Statistics on work zone safety show that, rear-end crashes, meaning those run into the rear of a slowing or stopping vehicle, are the most common type of work zone crash. Additional, majority of fatal work zone crashes occurred on roads with speed limits greater than 50 mph [2]. These two key facts, unfortunately, precisely describe the working environment of M&SMO workers. When performing M&SMO on freeway or highways, the general traffic usually travels at a speed that is higher than 50mph or even 70mph, while M&SMO vehicles are being operated between 5 and 15mph. The dramatic speed difference requires drivers of the conventional vehicles to timely assess the changing driving environment, rapidly perceive and respond by switching to a different lane or slowing down to avoid the potential crash. However, as research shows, aggressive driving and distracted driving happened very often and are the primary factors for work-zone crashes [3]. Additionally, driving under the influence of alcohol and/or drugs, performance of heavy vehicles, work zone length and traffic volume, speeding, dynamic traffic conditions, environmental conditions and many other factors also

contribute to the work zone crashes.

The Autonomous Maintenance Technology (AMT) is a quickly emerging autonomous-vehicle-based technology for improving transportation infrastructure maintenance by removing drivers from risk. The system, sometimes referred to as Autonomous Truck Mounted Attenuator (ATMA) or Autonomous Impact Protection Vehicles (AIPV), includes a leader truck (LT), a follower truck (FT), a truck mounted attenuator (TMA) installed on the FT, and a leader-follower system that enables the FT to drive autonomously and follow the LT. The leader-follower autonomous driving system includes actuators, software, electronics, and vehicle to vehicle (V2V) communication equipment that can be installed on Truck Mounted Attenuator-equipped LT and FT. While the LT is performing maintenance work, the FT is designed to serve as the buffer so if a rear-end crash is inevitable, the property damage can be minimized with the TMA hardware installed on the FT. The ultimate goal of this AMT system design is to remove DOT employees from the follower truck and eliminate injuries while performing slow moving operations [4].

Figure 1: AMT Vehicle System. (a) Front view, (b) Rear view

In 2017 the Colorado Department of Transportation (CDOT) launched the first AMT program in the US, with the goal of testing and deploying self-driving vehicles to increase work zone safety by

removing the driver from a truck that is designed to be hit. After that, CDOT started to lead an autonomous maintenance technology pool fund, which currently has 12 paid state DOT members. In 2018, Missouri DOT awarded a contract to purchase two AMT vehicles for work zone maintenance, with the goal of fully testing and deploying autonomous maintenance technology in Missouri. In 2019, University of Tennessee Center for Transportation Research announced a pilot demonstration to test and evaluate the potential for an autonomous system to improve work zone safety. Aside from Colorado and Missouri, the States that have purchased AMTA vehicles include at least California and Minnesota, and the number is increasing fast.

Before deploying AMT for work zone maintenance, one question that needs to be understood is how much impact AMT system cause to the transportation roadway capacity would. As roadway capacity describes the maximum amount of vehicular traffic that a particular roadway infrastructure can serve, the answer to this question would provide much-needed guidance to state DOT for transportation roadway maintenance-related work, as well as needed transportation performance management and system management. For example, if it turns out that additional traffic management plans were needed, or if the work zone maintenance should be done at a different time, informed decisions can be made ahead of time.

1.2 Objectives

The goal of this project is to study the impact of autonomous maintenance technology to transportation infrastructure capacity by developing models and algorithms to reveal the fundamental mechanism of AMT, and validating its accuracy with the field-collected data. This project provides much-needed guidance to state DOT for transportation roadway maintenance-related work, as well as needed transportation performance management and system management. This goal is closely relevant to the

thrust area 2 - “Monitoring: Condition monitoring, remote sensing, and the use of GPS for enhanced durability and life-extension of transportation infrastructure”, and thrust area 1 – “Management: Asset management and performance management for enhanced durability and life-extension of transportation infrastructure.”

1.3 Expected Contributions

Due to AMT vehicle’s nature of driving at a slow-moving speed (typically between 8 and 15mph), if its discount to the transportation infrastructure capacity is not corrected accounted, the maintenance work will cause significant amount of extra delay to the traffic flow that are operating on the transportation infrastructure. The derived capacity discount will deliver important practical values for DOT engineers to determine transportation roadway maintenance work timing, as well as to support their transportation performance management and system management efforts. The research team has presented the research outcomes at both national and local conferences, such as Transportation Research Board Annual Meetings and Missouri S&T Institute of Transportation Engineers seminars, to disseminate the research outcomes. The team has also presented two papers on TRB2020 annual meeting. Additionally, the PI was invited by the TRB AKR10 Committee on Maintenance and Operations Management for a national webinar on Autonomous Maintenance Technology in summer 2020, which attracted over 600 attendees from national wide.

1.4 Report Overview

This report is organized as follows. A literature review is provided in Section 2. Section 3 focuses on methodology development, in which the analytical derivations of the effective discharge rate for a four-lane highway segment is presented. In Section 4, the developed model is validated with a NGSIM dataset, and the modeling result analysis are discussed. Section 5 concludes this report.

Chapter 2. Literature Review

Due to its importance, work zone safety has received significant attentions over the last few decades, and many technologies have already been developed. For example, speed trailer was evaluated in Texas, in which speed profiles were obtained for passenger cars and trucks as they approached and traversed three rural high-speed work zones. The results showed that speed trailers and radar drones are effective in reducing the mean speed and percent of speeders in the work zones [5]. Ullman et al. documented the development of a field guide for portable changeable message sign, which played an important role in traffic control in work zones [6]. Usage of warning lights was also extensively documented. For example, Manual on Uniform Traffic Control Devices (MUTCD) recommended using of warning light on moving operation [7], and in [8] the usage of special flashing warning lights for construction, maintenance, and service vehicles was studied. Retro-reflective markings was shown to enhance visibility of work equipment at night under low traffic conditions, and Texas Transportation Institute (TTI) found that flagger vehicles with retro-reflective magnetic strips were useful to improve night visibility [9]. Other work zone technologies include portable changeable message signs, truck-mounted changeable message signs, potable highway advisory radio, zipper merge and many others.

TMAs are energy-absorbing devices attached to the rear of the trucks and used as protective vehicles, thus protecting the motorist and the protective vehicle's driver upon impact [10]. TMA has been in use by transportation agencies for many years, and usually are installed on a relatively heavy vehicle. For example, Missouri DOT requires the host vehicle to be at least 16,000 lbs [10], Texas DOT requires 20,000 lbs [11], and in Sweden this number is 9,000 kg (or 19,842lbs) [12]. While most transportation agencies are very familiar with TMA, trailer-mounted attenuators are increasing in popularity. TTI performed a systematic comparison between truck-mounted attenuators and trailer-mounted attenuators, from the perspectives of structural adequacy, occupant risk for the impacting

vehicle, and post-impact vehicular response. The researchers found that the concern of trailer-mounted attenuators swinging around may not be justified, given that post-impact trajectories of the impacting vehicles were similar to those reported during truck-mounted attenuator impact testing [11]. Additionally, three tests were performed and compared in [12], including a TMA on a tractor, a TMA on an articulated front-end loader and a TMA on a trailer. The research outcome recommended to allow certain types of alternative TMA carrier vehicles, under the condition that the vehicle weight limits were still met. A review of TMA application in work zones can be found in [13], in which five states were visited to solicit information regarding support for, and extent of use of, TMAs, and the results was summarized as the guidelines for the use of TMA in work zones.

ATMA is a quickly emerging technology that combines the usage of TMA and Connected and autonomous vehicles (CAV) in work zones. CAV has the great potential of changing our daily life and has attracted significant research attention recently. However, due to the complex roadway environment and other challenging issues, the question of when an autonomous vehicle could become fully functional in a real situation remained unanswered [14]. On the other hand, the application of CAV in a narrowly-defined and simplified environment, such as a work zone location with the lead-follower ATMA concept, becomes more realistic. Since its debut, ATMA has been receiving significant amount of attentions from state DOTs with the hope to reduce DOT employee's fatalities in work zones.

On the state of the practice of ATMA, in 2017 the Colorado Department of Transportation (CDOT) launched the first ATMA program in the US, with the goal of testing and deploying self-driving vehicles to increase work zone safety by removing the driver from a truck that is designed to be hit [15]. After that, CDOT started to lead an autonomous maintenance technology pool fund, which currently has 12 paid state DOT members [16]. In 2018, Missouri DOT awarded a contract to purchase two ATMA vehicles for work zone maintenance, with the goal of fully testing and deploying ATMA

technology in Missouri [17]. In 2019, University of Tennessee Center for Transportation Research announced a pilot demonstration to test and evaluate the potential for an autonomous system to improve work zone safety [18]. Aside from Colorado and Missouri, the States that have purchased AMTA vehicles include at least California and Minnesota and the number is increasing fast. However, to the best of our knowledge, our manuscript is the first academic research that focused on ATMA technology testing. As such, it is our hope to get the word out on early reliability of Autonomous TMAs, and we hope that this manuscript can serve as a reference for transportation agencies that are interested in deploying similar technologies.

Chapter 3. Methodology

3.1 Problem Setup

In this section, we focus on a typical highway with two lanes of the same direction, and the traffic on both lanes going to the right side, as shown in Figure 2. The ATMA vehicle system is represented by the two vehicles in the red box, with a leader truck (LT) and a follower truck (FT), and a gap distance of L_{gap} between these two vehicles. The other general vehicles are represented by a smaller black vehicle icon.

The total in-flow rate is $\lambda(t)$ for both lanes. The lane flow distribution is presented by α, so the left lane has a flow rate of $\alpha * \lambda(t)$, whereas the right-lane has a flow rate of $(1-\alpha) * \lambda(t)$. The cruising speed of general traffic is v_{u}, and ATMA vehicles drive at a constant speed of v_{lt} (with lt standing for leader truck). v_{lt} is usually between 5~15mph and is, thus, much slower than v_{u}, i.e., $v_{\text{lt}} < v_{\text{u}}$ and, as such, the ATMA can be considered as a moving bottleneck in the two-lane highway segment. As a result, the vehicles behind the ATMA vehicles (represented by red colored small cars in Figure 2) can switch to the left lane to bypass the moving bottleneck. Note that, although for simplicity a two-lane highway is used, the proposed model can be iteratively applied to a highway with three or even more lanes.

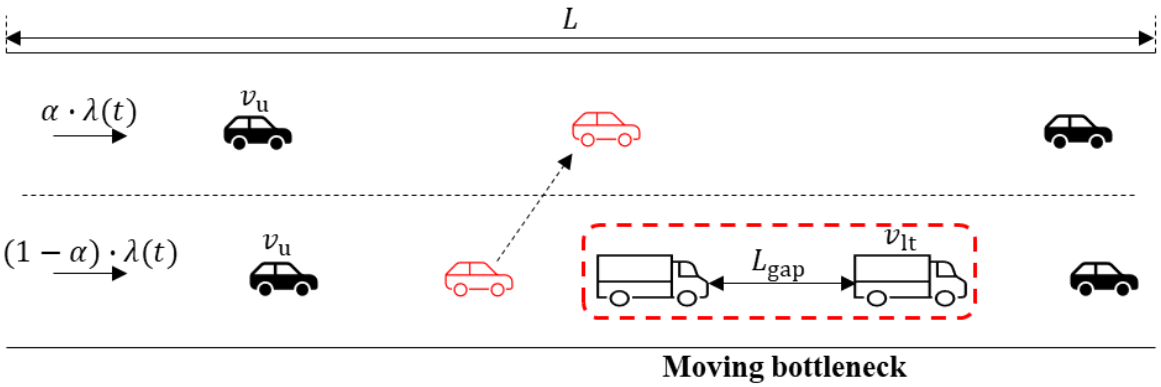

Figure 2. Schematic diagram of a four-lane highway (one direction) segment with ATMA vehicles.

3.2 Discharge Rate Under Normal Traffic Conditions

In this subsection, we review how to derive the discharge rate (i.e., highway capacity) under normal traffic conditions. A simplified car-following model was proposed by Newell [19] and adopted in this manuscript to describe a vehicle's kinematic movements on a roadway segment. The simplified model states that the time-space trajectory of a following vehicle n is essentially the same as its leading vehicle $n-1$, except for a delay in space and in time. In the time-space diagram (shown in Figure 3-a below), a leading vehicle $n-1$ initially drives at a constant speed v_1 and then changes to another constant speed v_2. According to the simplified car-following model, the following vehicle n also travels at the same speed of v_1 at the beginning, and then changes to the v_2 speed. However, at the turning point, there is a temporal delay of τ_n which represents the driver n's necessary response time, as well as a spatial delay of d_n, which represents the distance needed to ensure safe driving.

Following vehicle n's movement trajectory can be calculated by $x_n(t+\tau_n) = x_{n-1}(t) + d_n$. Based on the time-space diagram, the time headway of n's vehicle, before and after speed change, can be derived with $h_{n,1} = \tau_n + \frac{d_n}{v_1}$ and $h_{n,2} = \tau_n + \frac{d_n}{v_2}$, respectively. The space headway of n's vehicle, before and after the speed changes, can be computed by $s_{n,1} = d_n + \tau_n \cdot v_1$ and $s_{n,2} = d_n + \tau_n \cdot v_2$, respectively.

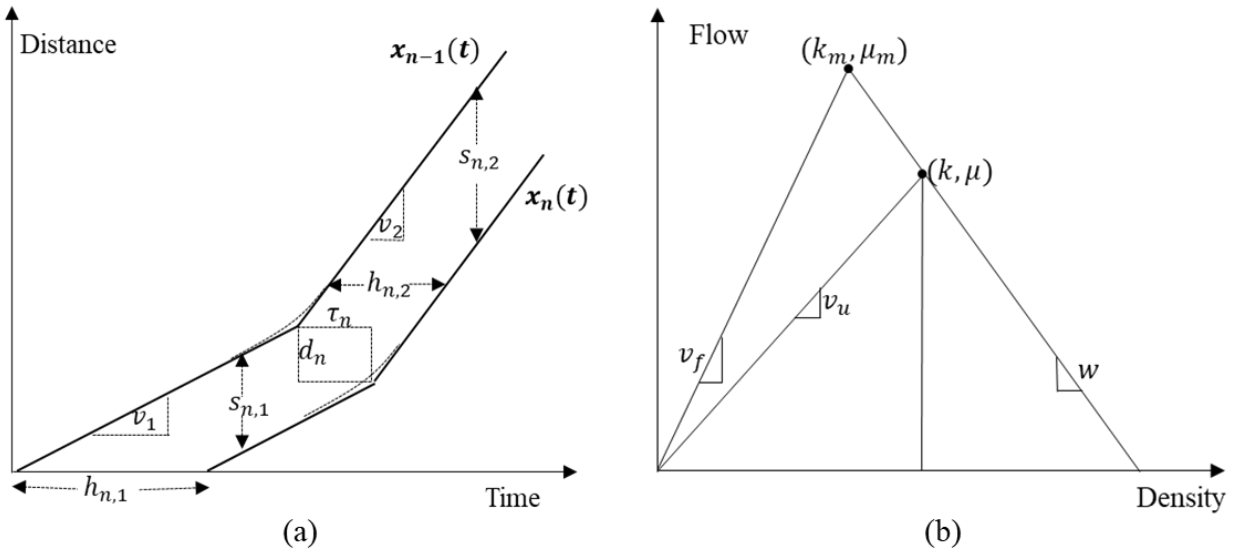

Figure 3. (a) Time-space diagram of Newell's car-following model and (b) triangular fundamental diagram.

The Newell car-following model above suggests the triangular fundamental diagram that is shown in Figure 3-b. Per [19], the q-k relationship can be represented as $q = \frac{1}{\bar{\tau}} - \frac{\bar{d}}{\bar{\tau}}k$, in which $\bar{\tau} = \frac{1}{n}\sum_{k=1}^{n}\tau_k$ and $\bar{d} = \frac{1}{n}\sum_{k=1}^{n} d_k$.The fundamental diagram has a free flow speed v_f, backward wave speed w, maximum discharge rate μ_m and its corresponding density k_m, and jam density k_j. Of the five variables, if three of them are known, the remaining two can be derived.

Following the above-mentioned fundamental diagram, when v_f, w, and k_j are known for a roadway segment, its maximum discharge rate μ_m can be calculated as $\mu_m = \frac{k_j}{(\frac{1}{v_f}+\frac{1}{w})} = \frac{k_j \cdot v_f \cdot w}{v_f + w}$. It should be noted that μ_m is the maximum discharge rate under prevailing traffic conditions. In the case of congestion (e.g., due to lane drop or other geometric reasons), the actual cruising speed may be lower than the free-flow speed. We used a new point (k, μ) in the q-k diagram in Figure 3-b to represent the discharge rate due to the congestion impact, with $\mu < \mu_m$. The cruising speed is denoted as v_u, with $v_u < v_f$, the new discharge rate becomes Eq.(1) in a generic form.

$$\mu = \frac{k_j}{(\frac{1}{v_u} + \frac{1}{w})} = \frac{k_j \cdot v_u \cdot w}{v_u + w} \quad (1)$$

3.3 Derivation of Discounted Capacity with Moving Bottleneck

Next, we will analytically derive the discounted capacity (or, effective discharge rate), influenced by this moving bottleneck. We follow the theory from Newell [20], that a moving coordinate system, traveling at speed v_{lt}, can be transformed into a corresponding analysis of flow past a stationary bottleneck, with some proper coordinate transformation.

We start by placing a "moving observer" on the main road who is traveling at the same velocity v_{lt} as the ATMA vehicles, at any time t, at a location $x^*(t)$ relative to the ATMA vehicles. The equation from Newell [20], on the derivation of $x^*(t)$, is given in Eq. (2). In our problem, since they travel at the same speed, $x^*(t)$ remains a constant. Next, we also place a "stationary observer" on the main road, whose location does not change.

$$x^*(t) = x(t) - v_{\text{lt}} \cdot t \quad (2)$$

As the moving observer moves at the same speed as the ATMA vehicles, from his perspective, the two-lane roadway segment becomes a stationary section of road with only one lane for the other vehicles adjacent to ATMA vehicles. From his perspective, there is a lane reduction with a capacity drop. Some vehicles merge from two lanes to one lane, pass this bottleneck location, and then switch lanes to drive again on a two-lane roadway segment (again, please refer to the red vehicles in Figure 2). Let us call the view from the moving observer's perspective "moving coordinates", and that from the stationary observer's perspective "stationary coordinates". Based on such definitions, the target of this

section, i.e., the moving bottleneck capacity, is the maximum discharge rate from a stationary observer's perspective, with the presence of ATMA vehicles. Below we show how to derive such a value step by step.

Assume that the flow and the density of the one lane and two lanes have a functional relationship in the stationary coordinates, i.e. $q = Q_1(k)$ and $q = Q_2(k)$, if we use $q^*(t)$ to denote the rate at which vehicles on the main road pass the moving observer, who is travelling at a speed of v_{lt}, then

$$q^*(t) = q - k \cdot v_{\mathrm{lt}} \tag{3}$$

The density of the one-lane and the two-lane roadway segments are the same, no matter whose perspective (moving observer or stationary observer) is adopted. The relationship between $q^*(t)$ and k can be derived as:

$$q^*(t) = Q_1(k) - k \cdot v_{\mathrm{lt}} = {Q_1}^*(k), \qquad q^*(t) = Q_2(k) - k \cdot v_{\mathrm{lt}} = {Q_2}^*(k) \tag{4}$$

In which ${Q_1}^*(k)$ and ${Q_2}^*(k)$ represent the q-k relationship of a one-lane and a two-lane roadway segment, as seen from the moving observer's perspective.

Figure 4 presents q-k fundamental diagrams of a one-lane and a two-lane roadway from both a moving observer's and a stationary observer's perspectives. The moving observer's view is marked with red (i.e., OGI), and the stationary observer's view is marked with black (i.e., $OG'I'$). The moving bottleneck's speed is fixed at v_{lt}. We start by noting that the triangle O-F-L is the fundamental diagram of the one-lane segment, and triangle O-G-I is the fundamental diagram of the two-lane segment in the moving coordinate. As discussed by Newell [20], if we add a flow of $k \cdot v_{\mathrm{lt}}$ to q^*, the resulting FD will be in the stationary coordinates. As such, the triangle O-F'-L' is the fundamental diagram of the one-lane segment and triangle O-G'-I' is the fundamental diagram of the two-lane segment in the stationary

coordinates. We have the angle of $\angle G'OI' = arctan\, v_{\mathrm{u}}$, angle of $\angle I'OI = arctan\, v_{\mathrm{lt}}$, and the angle of $\angle G'I'O = arctan\, w$.

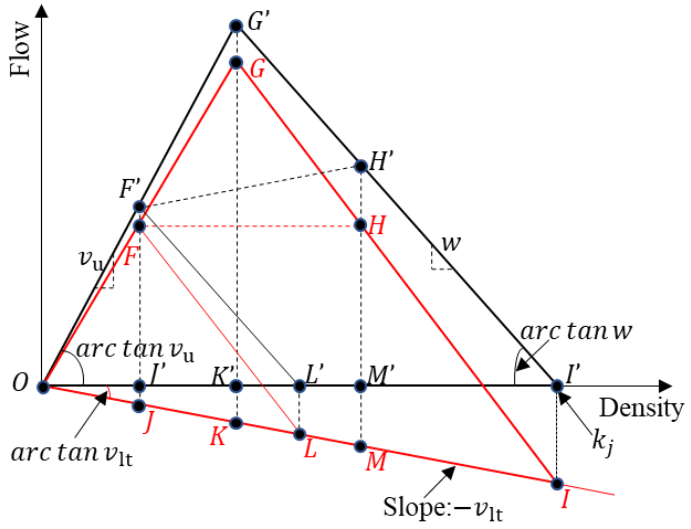

Figure 4. Flow-density relationship from both a moving observer's view and a stationary observer's view.

We first calculate the adjusted flow rate ${\lambda_{in}}'(t)$ in the moving coordinate system. At any given time t, we have an incoming flow rate $\lambda_{in}(t)$ and the moving bottleneck's speed v_{lt}. To convert that into the adjusted flow rate ${\lambda_{in}}'(t)$ in the moving coordinate system, we back calculate the density on the two-lane roadway segment with $Q_2(\,k_2) = \lambda_{in}(t)$, or $k_2 = {Q_2}^{-1}\big(\lambda_{in}(t)\big)$. Then, the adjusted flow rate ${\lambda_{in}}'(t)$ can be calculated as

$$ {\lambda_{in}}'(t) = \lambda_{in}(t) - k_2 \cdot v_{\mathrm{lt}} = \lambda_{in}(t) - {Q_2}^{-1}\big(\lambda_{in}(t)\big) \cdot v_{\mathrm{lt}} \qquad (5) $$

For example, in the stationary coordinate system, $F'J'$ is the maximum discharge rate of the one-lane segment, in which $F'J'$ is perpendicular to OI' and OJ' is its corresponding density. Following this with Eq.(5), to calculate the maximum discharge rate of the one-lane segment in the moving coordinate system, we need to reduce $F'J'$ by $OJ' \cdot v_{\mathrm{lt}}$ which is JJ' and, thus, becomes FJ'. In other words, FJ' is the maximum discharge rate of the one-lane segment in the moving coordinate system.

In the moving coordinate system, if $\lambda_{in}{}'(t) < FJ'$, all vehicles can pass through the moving bottleneck at full cruising speed v_{u}. Otherwise, the adjusted arrival rate $\lambda_{in}{}'(t)$ becomes higher than the maximum discharge rate and, thus, the ATMA vehicles become a moving bottleneck, and the roadway segment is subject to a maximum discharge rate with a value of FJ'. Subsequently, the traffic state of the downstream bottleneck location is represented by point F, while that of the bottleneck upstream is represented by point H, which has the same outflow rate as point F (i.e., $y_F = y_H$,) but with a higher density due to the queue. When we convert the moving coordinates back to the stationary coordinates points, F and H become points F' and H', after adding a flow of $k \cdot v_{\mathrm{lt}}$, i.e. $y_{F'} = y_F + k_F v_{\mathrm{lt}}$ and $y_{H'} = y_H + k_H v_{\mathrm{lt}}$. Since the density at point H is higher than that at point F (i.e., $k_H > k_F$), the flow rate at point H' is also higher than that at point F' (i.e., $y_{H'} > y_{F'}$), Thus, it is point H' that determines the maximum discharge rate, instead of point F' in the stationary coordinate system.

Next, we derive the length of $H'M'$, which is the maximum discharge rate of point H' in the stationary coordinate system (i.e., our target capacity with a moving bottleneck). First, let us look at the triangle of F-O-L, which is the fundamental diagram of a one-lane roadway. As $F'J'$ is the maximum discharge rate of the one-lane segment, we have $F'J' = \frac{\frac{k_j}{2}}{(\frac{1}{v_{\mathrm{u}}}+\frac{1}{w})} = \frac{k_j \cdot v_{\mathrm{u}} \cdot w}{2(v_{\mathrm{u}}+w)}$. As the angle of $\angle G'OI' = arctan\, v_{\mathrm{u}}$, OJ' can be calculated as $OJ' = \frac{F'J'}{v_{\mathrm{u}}} = \frac{k_j \cdot w}{2(v_{\mathrm{u}}+w)}$. As the angle of $\angle G'I'O = arctan\, w$, $J'L'$ can be calculated as $J'L' = \frac{F'J'}{w_m} = \frac{k_j \cdot v_{\mathrm{u}}}{2(v_{\mathrm{u}}+w)}$. As the angle of $\angle I'OI = arctan\, v_{\mathrm{lt}}$, JJ' can be calculated as $JJ' = OJ' \cdot v_{\mathrm{lt}} = \frac{k_j \cdot w \cdot v_{\mathrm{lt}}}{2(v_{\mathrm{u}}+w)}$. Then, the maximum discharge rate of the moving bottleneck in the moving coordinates with a value of FJ' can be calculated as

$$FJ' = F'J' - JJ' = \frac{k_j \cdot v_{\mathrm{u}} \cdot w}{2(v_{\mathrm{u}} + w)} - \frac{k_j \cdot w \cdot v_{\mathrm{lt}}}{2(v_{\mathrm{u}} + w)} = \frac{k_j \cdot w \cdot (v_{\mathrm{u}} - v_{\mathrm{lt}})}{2(v_{\mathrm{u}} + w)} \tag{6}$$

However, what we really need to calculate is the maximum discharge rate of point H' in the stationary coordinates, i.e., the length of $H'M'$. In the moving coordinates, we have the same flow at points F and H, which means that $HM' = FJ' = \frac{k_j \cdot w \cdot (v_{\mathrm{u}} - v_{\mathrm{lt}})}{2(v_{\mathrm{u}} + w)}$. As $G'K'$ is the maximum discharge rate of the two-lane segment, we have $G'K' = \mu_m = \frac{k_j}{(\frac{1}{v_{\mathrm{u}}} + \frac{1}{w})} = \frac{k_j \cdot v_{\mathrm{u}} \cdot w}{v_{\mathrm{u}} + w}$, and as the angle of $\angle G'I'O = arctan\, w$, $K'I'$ can be calculated as $K'I' = \frac{G'K'}{w} = \frac{k_j \cdot v_{\mathrm{u}}}{v_{\mathrm{u}} + w}$.

Suppose the density at point H' is k, we have $w = \frac{H'M'}{M'I'} = \frac{HM' + kv_{\mathrm{lt}}}{k_j - k} = \frac{\frac{k_j \cdot w \cdot (v_{\mathrm{u}} - v_{\mathrm{lt}})}{2(v_{\mathrm{u}} + w)} + kv_{\mathrm{lt}}}{k_j - k}$ and, thus, the density at point H' can be calculated as $k = \frac{k_j \cdot w}{2}(\frac{1}{v_{\mathrm{u}} + w} + \frac{1}{v_{\mathrm{lt}} + w})$. The effective discharge rate of point H' in the stationary coordinates, i.e., the length of $H'M'$can be calculated via Eq. (7).

$$\begin{aligned} \mu' = H'M' = HM' + kv_{\mathrm{lt}} &= \frac{k_j \cdot w \cdot (v_{\mathrm{u}} - v_{\mathrm{lt}})}{2(v_{\mathrm{u}} + w)} + \frac{k_j \cdot w \cdot v_{\mathrm{lt}}}{2}\left(\frac{1}{v_{\mathrm{u}} + w} + \frac{1}{v_{\mathrm{lt}} + w}\right) \\ &= \frac{k_j \cdot v_{\mathrm{u}} \cdot w}{v_{\mathrm{u}} + w} \cdot \frac{2v_{\mathrm{lt}} \cdot v_{\mathrm{u}} + w \cdot v_{\mathrm{u}} + w \cdot v_{\mathrm{lt}}}{2(v_{\mathrm{lt}} + w) \cdot v_{\mathrm{u}}} \\ &= \mu \cdot \frac{2v_{\mathrm{u}} \cdot v_{\mathrm{lt}} + v_{\mathrm{lt}} \cdot w + w \cdot v_{\mathrm{u}}}{2(v_{\mathrm{lt}} + w) \cdot v_{\mathrm{u}}} \end{aligned} \tag{7}$$

In this way, the effective discharge rate of the moving bottleneck in the stationary system in Figure 4 has now been derived. If we use a new variable θ and make $\theta = \frac{2v_{\mathrm{u}} \cdot v_{\mathrm{lt}} + v_{\mathrm{lt}} \cdot w + w \cdot v_{\mathrm{u}}}{2(v_{\mathrm{lt}} + w) \cdot v_{\mathrm{u}}}$, Eq. (7) becomes $\mu' = \mu \cdot \theta$, in which θ is, essentially, the capacity discount factor due to the moving bottleneck caused by the ATMA. In other words, before the ATMA vehicles enter the road, the roadway capacity is μ, and as soon as the ATMA vehicles enter the roadway segment, it creates a moving bottleneck with an

effective discharge rate of μ', given by Eq. (7), until the ATMA vehicles depart the roadway segment.

Chapter 4. NUMERICAL ANALYSIS

To validate the effective discharge rate discount factor equation that is derived in Eq. (7), the NGSIM dataset is used. This is because the validation of roadway capacity model requires information on all vehicles on the roadway segment and, as such, the NGSIM dataset (which includes high-resolution trajectory of every single vehicle) becomes the ideal dataset to use. We focus on the dataset for Northbound I-80 in Emeryville, California (shown in Figure 5). The study target includes lane 5 and lane 6, with a length of approximately 1,090 ft.

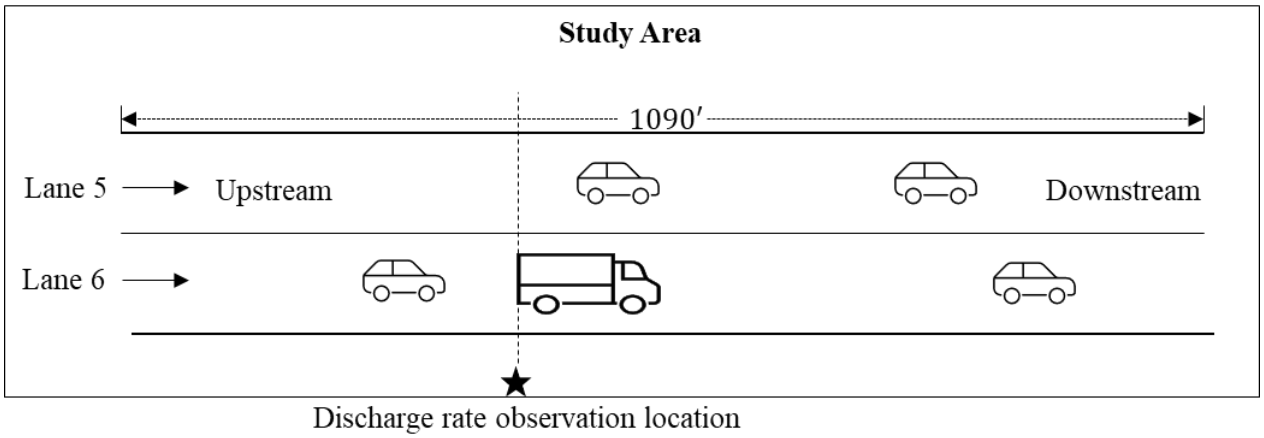

Figure 5. An illustration of the study area: Northbound I-80.

An open-source software, DTALite/NeXTA [21], is used to import NGSIM vehicle trajectories and to extract jam density, backward wave speed, and other needed characteristics. For the analyzed scenario, the vehicle trajectories in a time-space diagram for lane 5 and lane 6, between 04:00 p.m. and 04:15 p.m., and between 05:00 p.m. and 05:30 p.m. on April 13, 2005, are used. Figure 6 below illustrates the vehicle trajectories in a time space diagram for lanes 5 and 6. The areas highlighted by red rectangles A~E show the shockwave propagation in the NGSIM dataset. The slopes of these shockwaves range from 10 mph to 14 mph and, as such, the average backward wave speed is set at 12

mph. The jam density is set as 180 veh/lane/mile, and a cruising speed of 30 mph is used. According to Eq.**(1)**, the maximum discharge rate of the traffic stream can be calculated as $\mu = \frac{2k_j \cdot v_u \cdot w}{v_u + w} =$ 3,076 veh/hr.

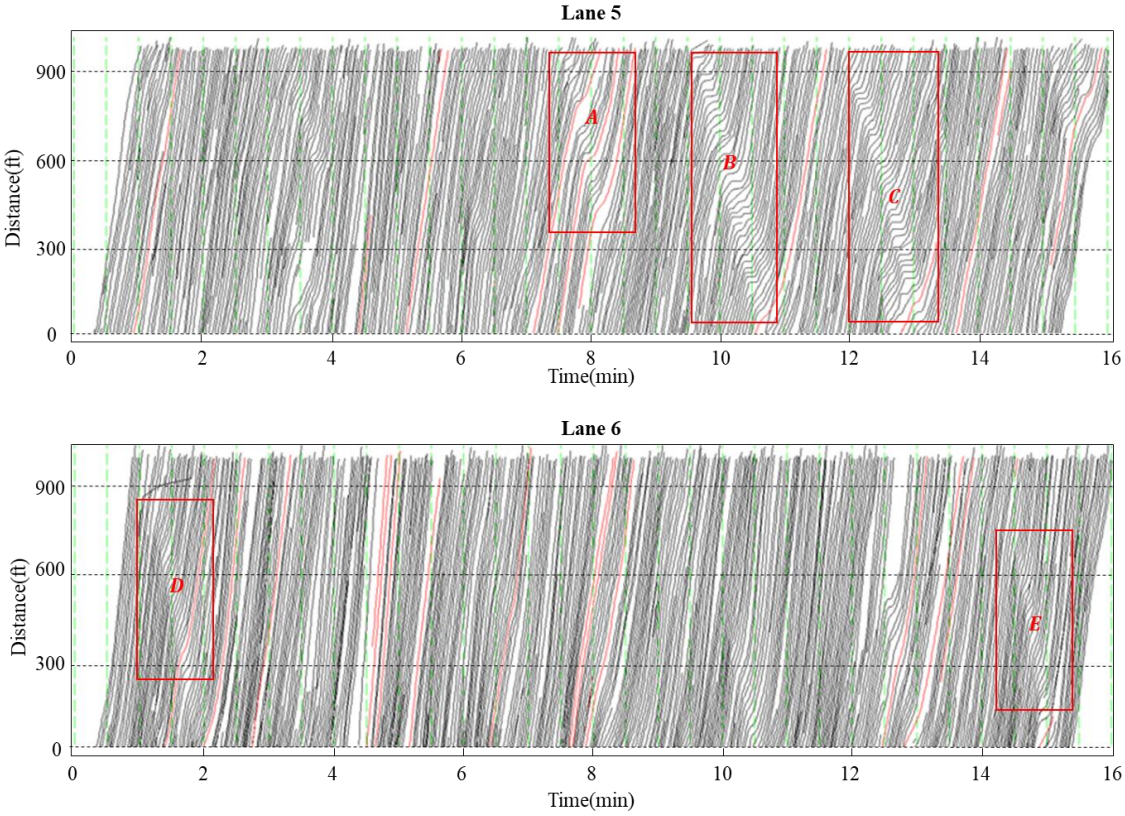

Figure 6. Vehicle trajectory for lanes 5 and 6, I-80, NGSIM.

To validate the effective discharge rate, we need to collect the ground truth discharge rate when affected by a moving bottleneck. To do so, we choose a fixed location (as shown by the star in Figure 5) as the location for observation. A total of six slow-moving trucks are observed on lane 5 and lane 6, between 04:00 p.m. and 04:15 p.m., and between 05:00 p.m. and 05:30 p.m. In other words, we observed a total of six moving bottlenecks. The time-space diagrams of two representative moving bottlenecks, generated by two slower trucks with ID 2862 and 1522, are shown in Figure 7, in which red curves represent trucks, and black curves stand for other general vehicles. For the sake of simplicity, we

only show the time-space diagram of two trucks below.

In Figure 7 (a), the slower truck (ID: 2862) is driving in lane 6 at a travel speed of 11 mph. Based on the time-space diagram of lane 6, we can tell the slope of the truck trajectory is lower than that of the other vehicles, indicating that the truck is moving slower than the surrounding traffic. It can also be found that the vehicle that follows this truck has a broken trajectory in lane 6, meaning that it chooses to switch to the left lane in order to bypass the slow-moving bottleneck. Based on the time-space diagram, the ground truth discharge rate is found to be approximately 2,740 veh/hr, for lanes 5 and 6 combined. In other words, $\mu_{GTD} = 2{,}740$ veh/hr. According to Eq. (7), the discount factor of the effective discharge rate can be calculated as $\theta = 0.83$, and the effective discharge rate is $\mu' = 2{,}568$ veh/hr. Comparing μ' and μ_{GTD}, the absolute percentage error (APE) can be calculated as $APE_1 = \frac{|2{,}568-2{,}740|}{2{,}740} = 6.3\%$. On the other hand, if we ignore the impact of the moving bottleneck and directly use the maximum discharge rate μ, by comparing μ and μ_{GTD}, the APE would become $APE_2 = \frac{|3{,}076-2{,}740|}{2{,}740} = 12.3\%$. Comparison of APE_1 and APE_2 suggests that using the proposed effective discharge rate is more reasonable than directly using the maximum discharge rate, and the resulting APE drops from 12.3% to 6.3%.

Figure 7 (b) presents the time space diagram of the moving bottleneck generated by another slower truck (ID: 1522) with a traveling speed of 5 mphr. The ground truth discharge rate can be observed and approximately equals $\mu_{GTD} = 1{,}982$ veh/hr. The effective discharge rate can be calculated as $\mu' = 2{,}127$ veh/hr. Thus, the APE can be calculated as $APE_1 = \frac{|2{,}127-1{,}982|}{1{,}982} = 9.5\%$, when compared with the ground truth discharge rate. However, the APE will become $APE_2 = \frac{|3{,}076-1{,}982|}{1{,}982} = 55.2\%$ if the impact of the moving bottleneck is ignored. The resulting APE drops from 55.2% to 9.5%, a significant improvement.

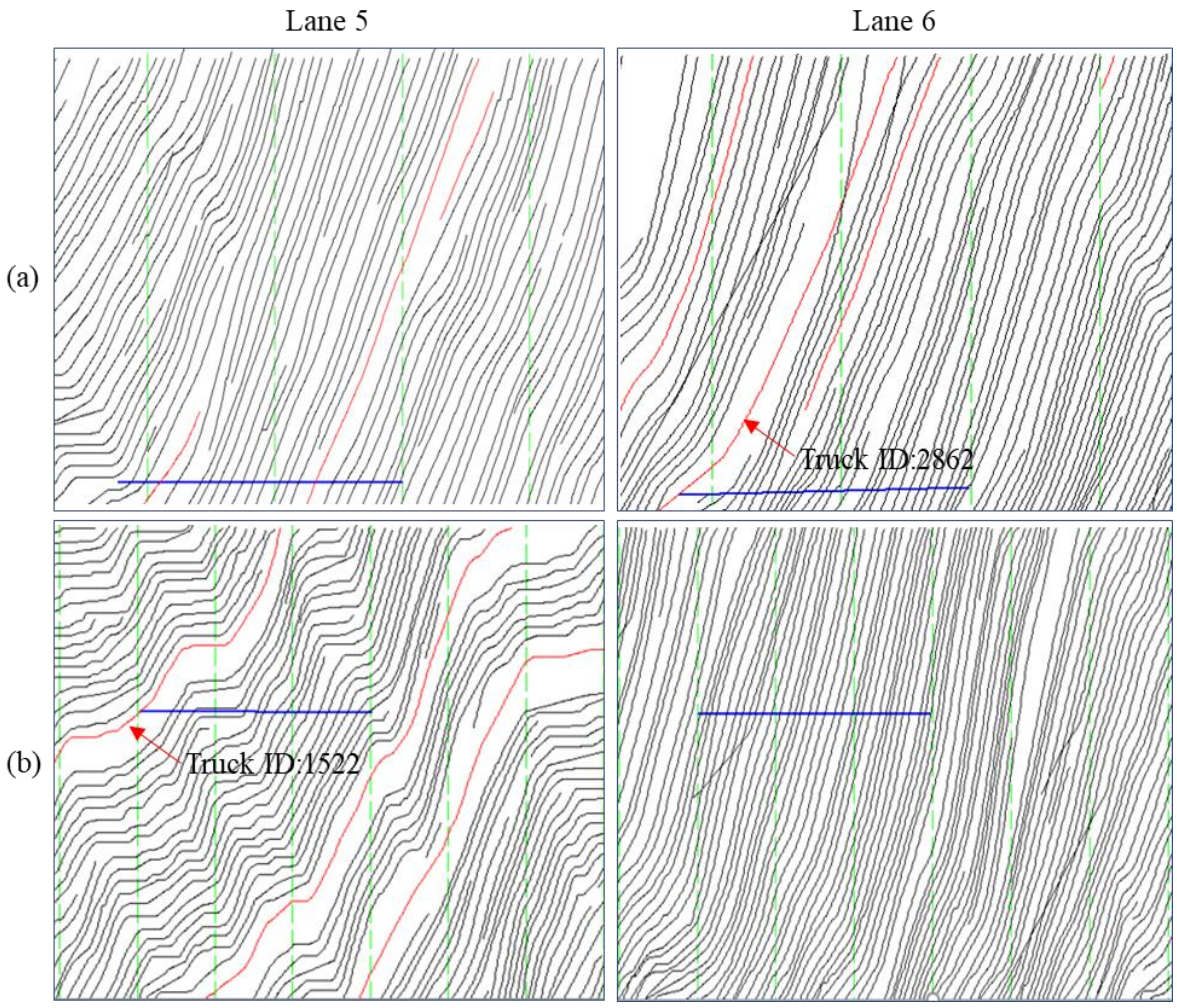

Figure 7. Vehicle trajectory of trucks (IDs:2862 and 1522), I-80, NGSIM.

Figure 8 shows the APE comparison of all six moving bottlenecks caused by those slow-moving trucks. It can be found that the maximum discharge rate μ (represented by the red solid line) always overestimates the ground truth discharge rate μ_{ground} (the black line), with APE_2 (the red dashed line) ranging from 12.3% to 55.2%. On the other hand, the proposed model can calibrate the effective discharge rate μ' (the blue solid line) much closer to the ground truth discharge rate μ_{ground}, with APE_1 (the blue dashed line) ranging from 6.3% to 13.6%. These numbers demonstrate that the proposed model can generate satisfactory traffic capacity associated with moving bottlenecks in traffic flow.

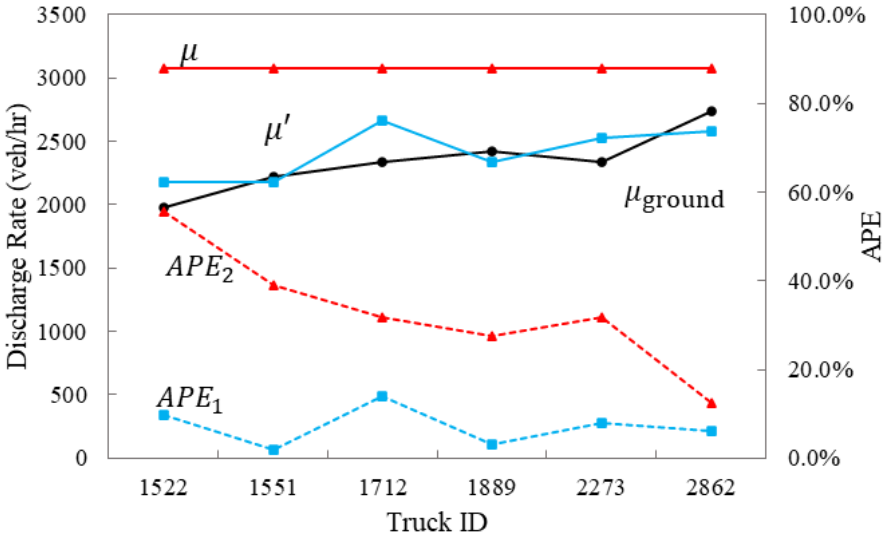

Figure 8. APE comparison of six slower trucks, I-80, NGSIM.

Chapter 5. Summary and Conclusions

This research project aims to mathematically derive the roadway capacity while an AMTA vehicle system is in operation, for transportation infrastructure maintenance on multilane highways, and at work zones. The effective discharge rate of a roadway segment is analytically derived, considering the moving bottleneck cause by slow-moving ATMA vehicles. The formulation is based on the fundamental diagram with moving coordinates. The derived effective discharge rates are represented with simple mathematical expressions in a closed-form, and correctly account for the effects of demand inputs and real time traffic status, as well as traffic flow characteristics. Validation with NGSIM data shows that our model correctly captures the effective discharge rate discount affected by moving bottlenecks, that results in an estimation error ranging from 6.3% to 13.6%, indicating a satisfactory result.

References

1. Tang, Q., Y. Cheng, X. Hu, C. Chen, and Y. Song. *Field Testing and Evaluation of Leader-Follower Autonomous Truck Mounted Attenuator Vehicle System for Work Zone Maintenance*. In *99th Annual Meeting of Transportation Research Board*. 2020. Washington DC.
2. FHWA. *Work Zone Safety for Drivers*. 2019; Available from: https://safety.fhwa.dot.gov/wz/resources/fhwasa03012/.
3. Long, S., B.K. Smith, E.H. Ng, and C. Sun, *Work zone safety: physical and behavioral barriers in accident prevention*. 2014, Missouri. Dept. of Transportation. Division of Construction and Materials.
4. Tang, Q., Y. Cheng, and X. Hu. *Quantification of Traffic Impact by Leader-Follower Autonomous Truck Mounted Attenuator Vehicle System for Work Zone Maintenance*. In *99th Annual Meeting of Transportation Research Board*. 2020. Washington DC.
5. Carlson, P.J., M. Fontaine, H. Hawkins, K. Murphy, and D. Brown. *Evaluation of speed trailers at high-speed temporary work zones*. In *79th Annual Meeting of TRB, Washington, DC*. 2000.
6. Ullman, G.L., C.L. Dudek, and B.R. Ullman, *Development of a field guide for portable changeable message sign use in work zones*. 2005, Texas Transportation Institute, Texas A & M University System.
7. FHWA, *Manual on uniform traffic control devices (MUTCD)*. 2009, FHWA, DOT Washington, DC.
8. Ullman, G.L., *Special flashing warning lights for construction, maintenance, and service vehicles: Are amber beacons always enough?* Transportation research record, 2000. **1715**(1): p. 43-50.
9. Fontaine, M.D., P.J. Carlson, and H.G. Hawkins Jr, *Evaluation of traffic control devices for rural high-speed maintenance work zones: second year activities and final recommendations*. 2000, Texas Transportation Institute.
10. MoDOT. *Missouri DOT Engineering Policy Guide, Category 612 Impact Attenuators*. 2020; Available from: https://epg.modot.org/index.php/Category:612_Impact_Attenuators.
11. Theiss, L. and R.P. Bligh, *Worker safety during operations with mobile attenuators*. 2013, Texas. Dept. of Transportation. Research and Technology Implementation Office.
12. Wenäll, J., *Alternative TMA carriers: crash test with a tractor, an articulated front-end loader and a rigid frame*. 2010: Statens väg-och transportforskningsinstitut.
13. Humphreys, J.B. and T.D. Sullivan, *Guidelines for the Use of Truck-Mounted Attenuators in Work Zones.* Transportation Research Record, 1991(1304).
14. Qi, H., R. Dai, Q. Tang, and X. Hu, *Coordinated Intersection Signal Design for Mixed Traffic Flow of Human-Driven and Connected and Autonomous Vehicles.* IEEE Access, 2020. **8**: p. 26067-26084.

15. Descant, S. *Colorado DOT Launches Autonomous Vehicles to Improve Worker Safety*. 2017; Available from: https://www.govtech.com/fs/data/Colorado-DOT-Launches-Autonomous-Vehicles-to-Improve-Worker-Safety.html.

16. CDOT. *Autonomous Maintenance Technology (AMT) Pool Fund*. 2018; Available from: http://www.csits.colostate.edu/autonomous-maintenance-technology.html.

17. MoDOT, *Leader-Follower Truck Mounted Attenuator System Request for Proposal*. 2018, Missouri Department of Transportation: Jefferson City, Missouri.

18. Inc., R.T.E. *Autonomous TMA Truck to Provide Insights to TDOT for Improving Work Zone Safety*. 2019; Available from: https://www.prnewswire.com/news-releases/autonomous-tma-truck-to-provide-insights-to-tdot-for-improving-work-zone-safety-300951862.html.

19. Newell, G.F., *A simplified car-following theory: a lower order model.* Transportation Research Part B: Methodological, 2002. **36**(3): p. 195-205.

20. Newell, G.F., *A moving bottleneck.* Transportation Research Part B: Methodological, 1998. **32**(8): p. 531-537.

21. Zhou, X. and J. Taylor, *DTALite: A queue-based mesoscopic traffic simulator for fast model evaluation and calibration.* Cogent Engineering, 2014. **1**(1): p. 961345.